

This article was downloaded by:

On: 26 January 2011

Access details: *Access Details: Free Access*

Publisher *Taylor & Francis*

Informa Ltd Registered in England and Wales Registered Number: 1072954 Registered office: Mortimer House, 37-41 Mortimer Street, London W1T 3JH, UK



## Liquid Crystals

Publication details, including instructions for authors and subscription information:

<http://www.informaworld.com/smpp/title~content=t713926090>

### High pressure phase studies of some liquid crystalline cyclohexane derivatives by differential thermal analysis

J. Rübesamen<sup>a</sup>; G. M. Schneider<sup>a</sup>

<sup>a</sup> Lehrstuhl für Physikalische Chemie II, Fakultät für Chemie, Ruhr-Universität Bochum, Bochum, Germany

**To cite this Article** Rübesamen, J. and Schneider, G. M.(1993) 'High pressure phase studies of some liquid crystalline cyclohexane derivatives by differential thermal analysis', *Liquid Crystals*, 13: 5, 711 – 719

**To link to this Article:** DOI: 10.1080/02678299308026343

**URL:** <http://dx.doi.org/10.1080/02678299308026343>

PLEASE SCROLL DOWN FOR ARTICLE

Full terms and conditions of use: <http://www.informaworld.com/terms-and-conditions-of-access.pdf>

This article may be used for research, teaching and private study purposes. Any substantial or systematic reproduction, re-distribution, re-selling, loan or sub-licensing, systematic supply or distribution in any form to anyone is expressly forbidden.

The publisher does not give any warranty express or implied or make any representation that the contents will be complete or accurate or up to date. The accuracy of any instructions, formulae and drug doses should be independently verified with primary sources. The publisher shall not be liable for any loss, actions, claims, proceedings, demand or costs or damages whatsoever or howsoever caused arising directly or indirectly in connection with or arising out of the use of this material.

## High pressure phase studies of some liquid crystalline cyclohexane derivatives by differential thermal analysis

by J. RÜBESAMEN and G. M. SCHNEIDER\*

Lehrstuhl für Physikalische Chemie II, Fakultät für Chemie,  
Ruhr-Universität Bochum, D-4630 Bochum, Germany

(Received 10 August 1992; accepted 1 February 1993)

$T(p)$  phase diagrams for the mesomorphic compounds *trans*-4-*n*-butylcyclohexane-1-carboxylic acid 4-cyanophenyl ester (D4N), *trans*-4-*n*-pentylcyclohexane-1-carboxylic acid 4-*n*-pentylphenyl ester (D55), *trans*-4,4'-di-*n*-propyl-1,1'-bicyclohexyl-*cis*-4-carbonitrile (33CCN), *trans*-4-methoxy-4'-propyl-1,1'-bicyclohexane (3O1CCH) and *trans*-4-methoxy-4'-*n*-butyl-1,1'-bicyclohexane (4O1CCH) are presented. The experiments were performed using high pressure microcomputer-assisted differential thermal analysis equipment in the temperature range 300 to 500 K up to a maximum pressure of 8 kbar. Some special high pressure effects for liquid crystals, such as pressure-induced or pressure-limited phases and changes from monotropic to enantiotropic polymorphism were observed. For the correlation of the experimental results, an extension of the Simon equation was used; one of the regression parameters of the clearing curve equation was found to be correlated with the molecular structure of the liquid crystal substances under test.

### 1. Introduction

Liquid crystals often show pronounced polymorphism. By introduction of different functional groups or systematic variation of chain lengths, the stability and temperature ranges of mesomorphic phases can be influenced. From such studies, information about the intermolecular forces that give rise to the different phases can also be obtained.

A method used only rather sparsely up to now involves changing the density and thereby the intermolecular distances by a variation of pressure; for a review of high pressure effects on liquid crystals see, for example, Chandrasekhar and Shashidhar [1]. The present paper is concerned with systematic high pressure investigations up to 8 kbar of some selected liquid crystal materials using differential thermal analysis (DTA).

### 2. Experimental

#### 2.1. Apparatus and experimental procedure

The experiments were performed using a microcomputer-assisted DTA apparatus developed by Sandrock [2] and Bartelt [3]. Several modifications and improvements were made to make accessible the pressure range up to 10 kbar. For safety reasons, the whole apparatus was mounted in a bunker and can be supervised and controlled by a remote digital device; for details see Rübесamen [4].

The central part of the apparatus is the twin autoclave, constructed according to the shrink-fitting method. The temperature and differential temperature are measured

\* Author for correspondence.

using steel-sheathed thermocouples. During the measurements, the sample (typically 30 mg) is enclosed in a sample cup made of lead or indium. A tight measuring cell of this type is able to transmit the pressure and protect the sample from being contaminated by the pressure medium. This is essential, because otherwise the pressurizing fluid can be dissolved in the sample resulting in a change in the transition temperatures. Here argon gas has been used in all experiments. The calibration of the thermocouples was carried out internally with highly purified reference materials, using a procedure that was suggested by Höhne *et al.* [5] to improve standardization and comparison of the experimental results. The accuracy of the temperature measurements was  $\pm 0.5$  K, even at elevated pressures; in all experiments, heating rates of  $1 \text{ K min}^{-1}$  were used. No correction was necessary for the pressure effect on the thermocouples.

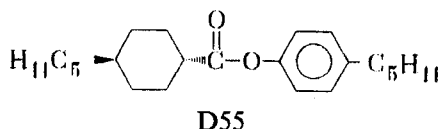
The thermal sensitivity was evaluated to be about 1 mJ per sample at atmospheric pressure. Because of the decrease of peak height of the DTA signal at high pressures that is caused by the rising heat conductivity of the pressure transmitting medium, a derivative DTA algorithm was used in a few cases for the determination of the transition temperature; this increases the above mentioned sensitivity to roughly some  $\mu\text{J}$ .

The pressure is measured by a high precision strain gauge and, up to 7 kbar, simultaneously by a Heise bourdon gauge. Both devices were calibrated against a 10 kbar pressure balance at the van der Waals Laboratory, University of Amsterdam (Netherlands). The accuracy of the pressure measurements was determined to be better than  $\pm 10$  bar. The details of the apparatus and of the experimental procedure are described elsewhere [4].

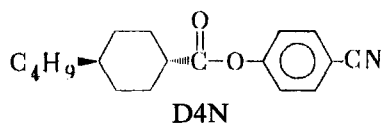
## 2.2. Samples under test

The selection of the samples under test results from a systematic continuation of the measurements made by Bartelt [6], who studied the influence of several functional groups on the phase behaviour of some liquid crystal materials. In the present work, additional structural elements were taken into consideration. In particular the following substances were investigated:

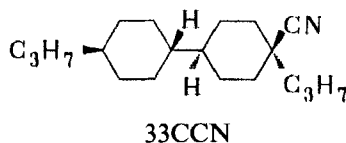
*trans*-4-*n*-pentylcyclohexane-1-carboxylic acid 4-*n*-pentylphenyl ester,



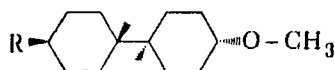
*trans*-4-*n*-butylcyclohexane-1-carboxylic acid 4-cyanophenyl ester,



*trans*-4,4'-di-*n*-propyl-1,1'-bicyclohexyl-*cis*-4-carbonitrile,



*trans*-4-methoxy-4-propyl-1,1'-bicyclohexane and *trans*-4-methoxy-4'-*n*-butyl-1,1'-bicyclohexane,



R

C<sub>3</sub>H<sub>7</sub> 3O1CCH

C<sub>4</sub>H<sub>9</sub> 4O1CCH

The substances under test were initially synthesized for display applications. They have high chemical and thermal stabilities and low transition temperatures at normal pressure. Therefore the transition temperatures are in the experimentally accessible region of the present apparatus even at elevated pressures. All substances were purchased from Merck AG, Darmstadt, Germany, and used without further purification.

### 3. Results

The results of the measurements are presented in figures 1 to 6. Here the metastability of a phase is marked by bracketing the phase symbol.

#### 3.1. D55

Figure 1 shows the  $T(p)$  phase diagram of D55. At normal pressure D55 undergoes two liquid crystal transitions. The clearing transition is 12 K above the melting transition, whereas at 7 K below the melting transition a change from the nematic to the S<sub>A</sub> phase occurs; this phase is monotropic with respect to the solid state and was only observed in cooling experiments, taking advantage of the pronounced supercooling of the melting transition.

#### 3.2. D4N

The second ester in this investigation is D4N. At normal pressure the registration curve of the melting transition showed a varying shoulder with low reproducibility. This effect indicates the existence of an additional, probably metastable phase; it could, however, not be stabilized by annealing experiments and was no longer observed at high pressure.

The phase diagram of D4N is shown in figure 2. Because of the small thermal effects and the increasing heat conductivity of the pressurizing medium at higher pressures, the values of the clearing temperatures at 2.71 and 4.09 kbar were determined by the derivative DTA method mentioned above.

The phase diagram of D4N exhibits only a nematic phase between the solid and the isotropic liquid state. The increase in the nematic range with pressure is more pronounced in the case of D4N than for D55, whereas the melting pressure curves of both substances are nearly parallel with each other, that for D4N being shifted to somewhat higher temperatures. Therefore the higher stabilization of the nematic phase of D4N with rising pressure is assumed to be an effect of the increase in the attractive forces involving the polar carbonitrile group that results in a higher density and packing, dimerization and increasing pressure working in the same direction for this substance.

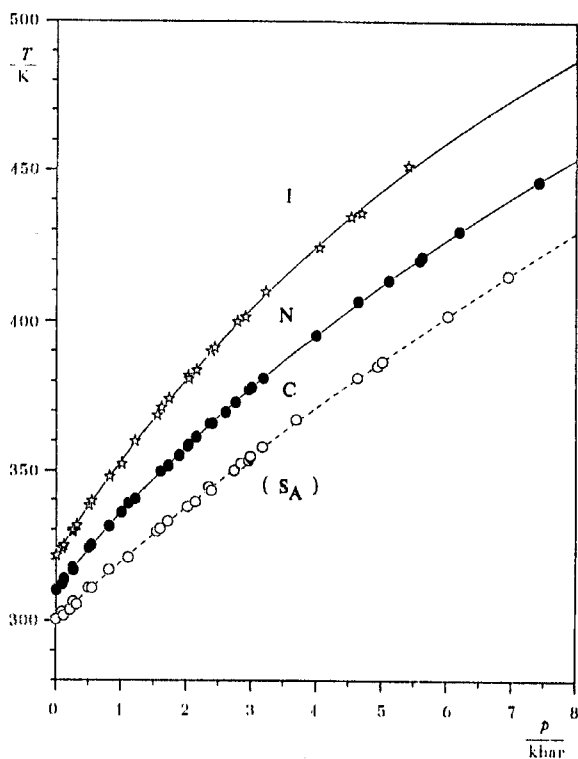


Figure 1. Phase diagram for D55. ●, Melting transition crystal (C)–nematic (N); ○, N–smectic A ( $S_A$ ) during cooling experiments; ☆, N–isotropic liquid (I).

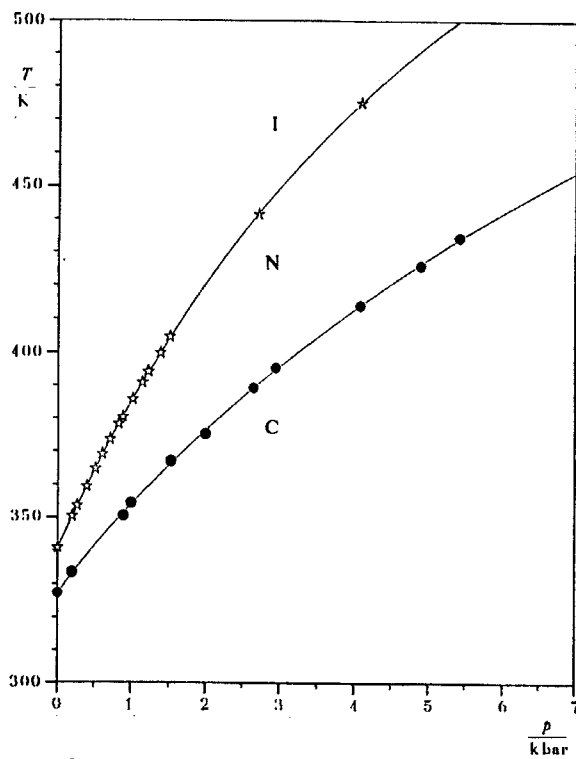


Figure 2. Phase diagram for D4N. ●, Melting transition C–N; ☆, N–I; ☆, N–I using a derivative DTA-algorithm for the determination of the transition temperature.

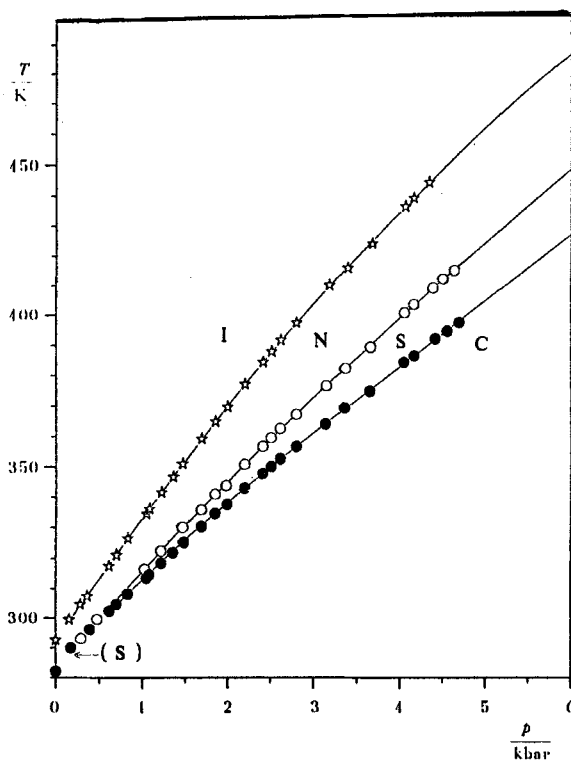


Figure 3. Phase diagram for 3O1CCH. ●, Melting transition C-N; ○,  $S_A$ -N; ☆, N-I.

### 3.3. 3O1CCH and 4O1CCH

In the case of 3O1CCH, two mesomorphic phases are known from the literature. The nematic phase is enantiotropic, whereas the smectic phase is metastable with respect to the solid phase. The determination of the transition temperatures at normal pressure was not unambiguous: from the measurements of the present work, a clearing temperature 4K higher than that given in the product information sheet of the manufacturer was obtained; Eidschink [7] and Kleeman [8] also found higher values.

The  $T(p)$  phase diagram obtained for 3O1CCH is presented in figure 3. In the temperature range below 300 K, an accurate determination of the transition temperature was not possible because these temperatures were below the calibration interval; therefore no regression curve is drawn in this region in figure 3.

Figure 3 demonstrates that the nematic phase is stabilized with increasing pressure. The smectic phase is also stabilized and even shifted from the metastable into the stable region. Below the triple point N-S-C, the N-S transition had to be detected in cooling experiments followed by subsequent heating sequences, taking advantage of the pronounced supercooling of the melting transition.

In figure 4 typical DTA traces for 3O1CCH at different pressures are given. They also demonstrate the stabilization of the nematic phase, as well as the appearance of the smectic phase with increasing pressure.

Figure 5 shows the  $T(p)$  phase diagram for 4O1CCH. Here the nematic phase has disappeared and only a smectic B phase exists.

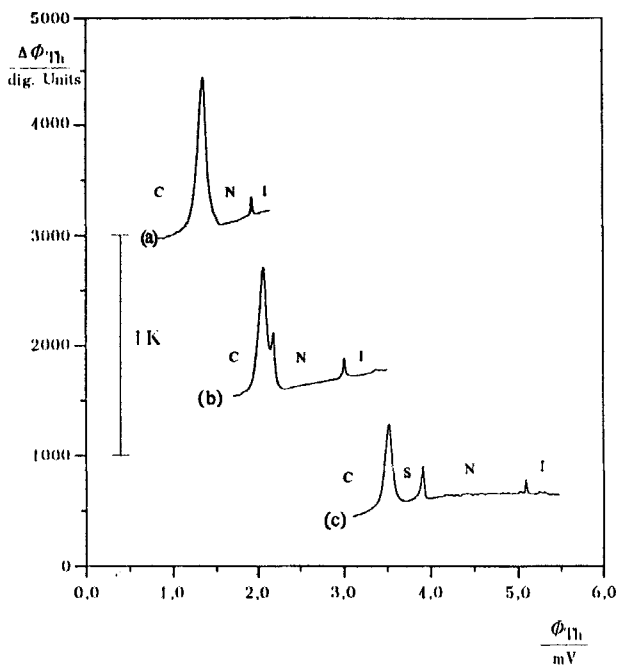


Figure 4. DTA traces for 3O1CCH. Plot of the differential temperature (electromotive force in digital units) against the temperature of a calibrated chromel/alumel thermocouple (electromotive force in mV). (a) 0.70 kbar, (b) 1.36 kbar, (c) 2.81 kbar.

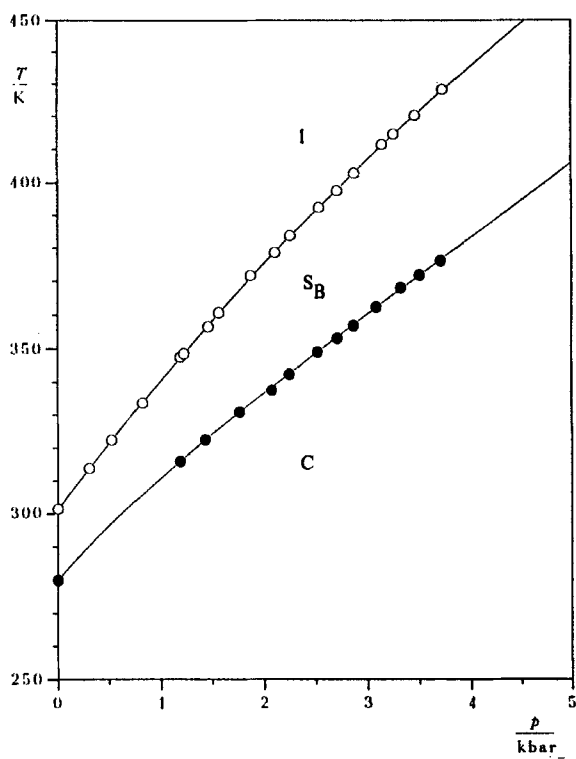


Figure 5. Phase diagram for 4O1CCH. ●, Melting transition C/S<sub>B</sub>, ○, clearing transition S<sub>B</sub>/I.

## 3.4. 33CCN

The  $T(p)$  phase diagram for 33CCN is given in figure 6. Here a nematic phase is found that is monotropic with respect to the crystal phase at normal pressure. With increasing pressure, however, it is shifted into the enantiotropic region and the  $T(p)$  curves of the clearing and melting transitions intersect at a triple point I-N-C at 2.1 kbar and 362 K. The  $T(p)$  phase diagram of 33CCN shown in figure 6 was extended to 15 kbar by Kleemann [9], using a diamond anvil cell technique.

33CCN differs from 3CCH, which has already been investigated at high pressures by Bartelt *et al.* [6], in the position of the carbonitrile group; it is equatorial in 33CCN, whereas in 3CCH it is axial. As a consequence of the equatorial position, no antiparallel association, such as that observed with 3CCH, takes place in the case of 33CCN [7]. Because of the lower length to width ratio in the non-associated 33CCN, the mesomorphic range of 3CCH is larger than that of 33CCN.

## 3.5. Extension of the Simon equation

In the literature, often empirical expressions (polynomials, etc.) are used for the correlation of the transition lines, for example the semi-empirical Simon equation. This equation can be derived from the well-known generalized Clausius-Clapeyron equation

$$\Delta H/\Delta V = T \cdot dp/dT = dp/d \ln T \approx \Delta p/\Delta \ln T \quad (1)$$

with the presumption that the quotient  $\Delta H/\Delta V$  is a linear function of pressure [10]; here  $T$  is the transition temperature,  $\Delta H$  and  $\Delta V$  the transition enthalpy and transition

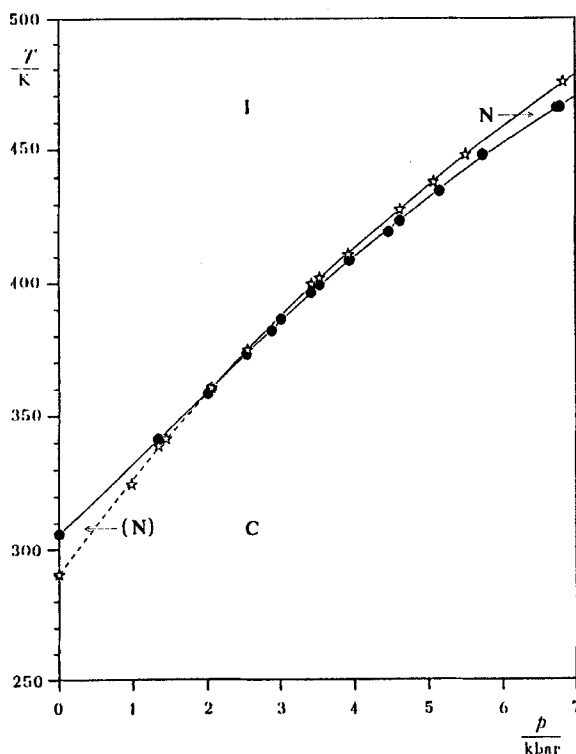


Figure 6. Phase diagram for 33CCN. ●, Melting transition C-I and C-N; ☆, clearing transition (N)-I and N-I.



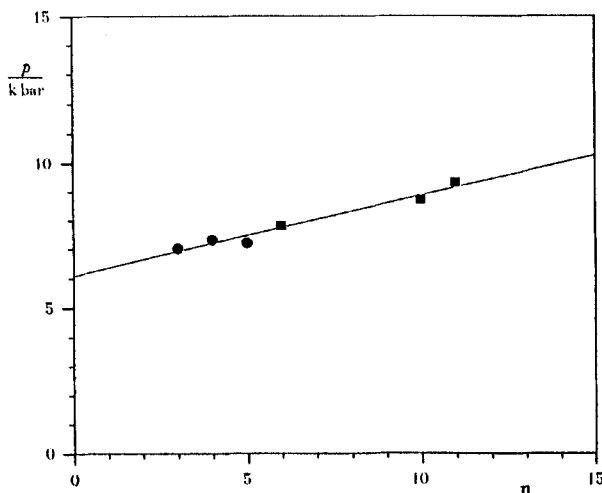


Figure 7. Plot of the parameter  $a$  of the expanded Simon equation (equation (2)) against the sum of carbon atoms ( $n$ ) in the alkyl chains for the clearing transition of the following mesogens: ■, 33CCN, 55CCN, 47CCN [4]; ●, 301CCH, 401CCH [4]; 501CCH [11].

volume, respectively. In the present study, this presumption was checked by plotting  $\Delta p/\Delta \ln T$  against  $p$  for some of the selected liquid crystal materials studied, for example, 33CCN. Since systematic deviations from straight lines were found, a quadratic approach was used as a first approximation:

$$\Delta H/\Delta V = a + b \cdot p + c \cdot p^2. \quad (2)$$

For details see Rübesamen [4].

Integration and some basic mathematical operations yield an extended Simon equation (see equation (3)), where  $q$  is the abbreviation for the term  $4 \cdot a \cdot c - b^2$ . Equation (3) is only valid for  $q > 0$

$$T(p) = T_0 \exp \left\{ \frac{2}{\sqrt{q}} \left[ \arctan \left( \frac{2 \cdot c \cdot p + b}{\sqrt{q}} \right) - \arctan \left( \frac{2 \cdot c \cdot p_0 + b}{\sqrt{q}} \right) \right] \right\}. \quad (3)$$

$T_0$  is the transition temperature at the pressure  $p = p_0$ , where  $p_0$  is in most cases equal to the normal pressure.

Equation (3) is able to reflect the influence of the chain length on the phase behaviour of the homologous series. The parameter  $a$  obtained by an iterative least squares fit of the clearing transition lines is plotted against the number of carbon atoms in the alkyl groups of some bicyclohexyl derivatives in figure 7. In the case of 33CCN [4] and 47CCN [4], the cyano group and, in the case of 301CCH, 401CCH and 501CCH [11], the methoxy group, were assumed to belong to the central molecular core. The plot in figure 7 shows a nearly linear dependence in the experimental range. This holds even for 401CCH, where the clearing transition takes place from the smectic B phase into the isotropic phase and not, as in all other cases, from the nematic phase. Some homologous series taken from the literature were also treated in an analogous way. In all cases studied, the parameters  $a$  show higher values for increasing alkyl chain lengths and consequently (slightly) increasing volumes (see [4]). The parameter  $a$  being inversely proportional to the initial slope of the transition line, this result gives a hint as to the commonly observed lowering of the pressure-induced

stabilization of the nematic range with increasing alkyl chain length [12, 13]; a (small) odd-even effect cannot be excluded (see [14]). No dependence on structure, however, could be found for the other transitions nor for the parameters  $b$  or  $c$ . For additional data and a detailed discussion see [4].

Financial support from the Deutsche Forschungsgemeinschaft (DFG) and the Fonds der Chemischen Industrie e.V. is gratefully acknowledged. The authors thank Merck AG, Darmstadt, Germany, for making available the liquid crystals materials investigated; they are indebted to Dr Schouten, van der Waals Laboratory, Amsterdam, The Netherlands, for the calibration of the manometers.

### References

- [1] CHANDRASEKHAR, S., and SHASHIDHAR, R., 1979, *Advances in Liquid Crystals*, Vol. 4, edited by G. H. Brown (Academic Press), p. 83.
- [2] SANDROCK, R., 1982, Doctoral Thesis, Ruhr-Universität Bochum, Germany.
- [3] BARTELT, A., and SCHNEIDER, G. M., 1989, *Rev. scient. Instrum.*, **60**, 926.
- [4] RÜBESAMEN, J., 1992, Doctoral Thesis, Ruhr-Universität Bochum, Germany (Verlag Shaker).
- [5] HÖHNE, G. W. H., CAMMENGA, H. K., EYSEL, W., GMELIN, E., and HEMMINGER, W., 1990, *Thermochim. Acta*, **160**, 1.
- [6] BARTELT, A., and SCHNEIDER, G. M., 1989, *Molec. Crystals liq. Crystals*, **173**, 75.
- [7] EIDENSCHINK, R., 1985, *Molec. Crystals liq. Crystals*, **123**, 55.
- [8] KLEEMANN, J., 1991 (private communication).
- [9] KLEEMANN, J., 1991, Doctoral Thesis, Ruhr-Universität Bochum, Germany.
- [10] UBBELOHDE, A. R., 1978, *The Molten State of Matter* (Wiley), Chap. 6, p. 19.
- [11] RITTMEIER-KETTNER, M. K., Doctoral Thesis, Ruhr-Universität Bochum, Germany (in preparation).
- [12] HERRMANN, J., KLEINHANS, H. D., and SCHNEIDER, G. M., 1983, *J. Chim. phys.*, **80**, 111.
- [13] SCHNEIDER, G. M., BARTELT, A., FRIEDRICH, J., REISIG, H., and ROTHERT, A., 1986, *Physica B*, **139** and **140**, 616.